

PAPER

View Article Online
View Journal | View IssueCite this: *J. Mater. Chem. C*, 2015, **3**, 5226

An indigo-based polymer bearing thermocleavable side chains for n-type organic thin film transistors†

Chang Guo, Jesse Quinn, Bin Sun and Yuning Li*

A new n-type semiconducting polymer based on indigo having thermocleavable *tert*-butoxycarbonyl (*t*-Boc) groups was synthesized and used as an active layer in organic thin film transistors (OTFTs). Twisting of the polymer main chain due to the presence of the bulky *t*-Boc groups renders this indigo-based polymer highly soluble. A post-deposition thermal treatment at a temperature above 170 °C could remove the *t*-Boc groups to retrieve the highly coplanar geometry of the unsubstituted indigo units. The thermally annealed polymer semiconductor films at 200 °C showed an electron mobility of up to $\sim 6 \times 10^{-3} \text{ cm}^2 \text{ V}^{-1} \text{ s}^{-1}$ in OTFTs, which is a 5-fold increase compared to that of the indigo-based polymers reported previously due to the retrieved high backbone coplanarity.

Received 23rd February 2015,
Accepted 13th April 2015

DOI: 10.1039/c5tc00512d

www.rsc.org/MaterialsC

Introduction

In the past decade, π -conjugated polymers have rapidly become promising semiconductor candidates for applications demanding low costs, large area, and flexibility, such as radio frequency identification (RFID) tags, displays, solar cells, and portable electronics.^{1–6} Recently, electron donor (D) and acceptor (A) moieties have been utilized for tuning the optoelectronic properties of conjugated polymers.^{4,7–12} The strong intermolecular interaction between donor and acceptor units is beneficial for shortening the π - π stacking distance and facilitates the self-assembly of polymer chains to form highly ordered chain packing and well-interconnected microstructures.^{13–15} Hence D–A polymers have shown very high charge carrier mobilities in organic thin film transistors (OTFTs). To maximize the performance of D–A polymers, novel electron acceptor building blocks with a coplanar geometry have been extensively explored.^{16–20}

Indigo derivatives, which are known commercial dyes,^{21,22} have recently attracted attention as semiconductors since they demonstrated good semiconductor performance in OTFTs.^{23–29} Previously we successfully used Tyrian purple (Fig. 1), a naturally occurring indigo dye, as an acceptor and bithiophene as a donor to construct D–A polymers.²⁷ Nitrogen atoms in Tyrian purple are suitable for substitution with acyl side chains to render the resulting polymers soluble. However, we found that the *N*-substitution

led to a large dihedral angle between two lactam units, causing serious twisting of the polymer backbone. In addition, *cis*-indigo units might exist due to the steric effect of the side chains. Consequently, zigzagged and twisted polymer main chain conformations would form, which limits electron delocalization. Therefore, if the solubilizing side chains on indigo could be recovered after the deposition of polymer thin films, the charge transport performance of indigo-based polymers is expected to improve.

Recently, Sariciftci *et al.* introduced a thermally labile protection group, *tert*-butoxy carbonyl (*t*-Boc) to indigo derivatives.²⁸ Upon thermal annealing at a moderately high temperature ($> 150^\circ\text{C}$), *t*-Boc groups were removed to regenerate the planar unsubstituted indigo moiety. Although this strategy is successful in solubilizing small indigo molecules, the solubility of the *t*-Boc substituted indigo-*co*-bithiophene polymer, poly(DTI), is

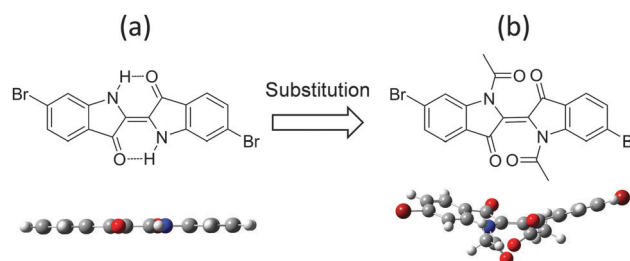


Fig. 1 The chemical structures and geometries of model compounds (a) Tyrian purple, (*E*)-6,6'-dibromo-[2,2'-biindolinyldiene]-3,3'-dione (*trans*-IDBr), and (b) the acetyl substituted Tyrian purple, (*E*)-1,1'-diacetyl-6,6'-dibromo-[2,2'-biindolinyldiene]-3,3'-dione (*trans*-IDBrAc). The molecular geometries were obtained by density functional theory (DFT) calculations (the details are provided in the ESI†).

Department of Chemical Engineering and Waterloo Institute for Nanotechnology (WIN), University of Waterloo, 200 University Ave West ON, Waterloo, N2L 3G1, Canada. E-mail: yuning.li@uwaterloo.ca; Fax: +1-519-888-4347; Tel: +1-519-888-4567 ext. 31105

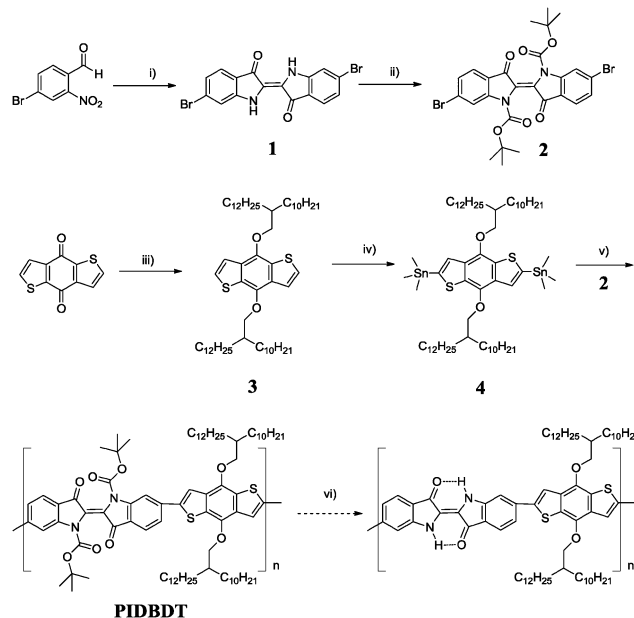
† Electronic supplementary information (ESI) available: Details of computer simulations, NMR, DSC, and additional OTFT data. See DOI: 10.1039/c5tc00512d

very poor. Nonetheless, they used a potentiodynamic electro-polymerization technique to prepare poly(DTI) films and observed the photoconduction effect of this polymer in diodes. In this study, we substituted Tyrian purple with *t*-Boc and copolymerized it with another monomer unit, benzo[1,2-*b*:4,5-*b'*]-dithiophene that bears bulky alkoxy side chains as a donor. The resulting polymer is readily solution processable. Upon thermal removal of the *t*-Boc groups, the indigo units of the resulting polymer become highly coplanar, affording promising electron transport performance in OTFTs.

Results and discussion

Tyrian purple has two functional bromo groups at the 6 and 6' positions, which can potentially be used as monomers for constructing polymers. Nevertheless, Tyrian purple shows extremely poor solubility in common organic solvents. Substitution at the nitrogen atoms of Tyrian purple with acyl groups could improve the solubility of the substituted Tyrian purple derivatives.²⁷ However, computer simulations of Tyrian purple (*trans*-IDBr) and the acetyl substituted Tyrian purple (*trans*-IDBrAc) using density functional theory (DFT) calculations with Gaussian 09W^{30,31} indicated that the acyl substitution caused serious twisting of the substituted Tyrian purple molecule (Fig. 1 and Table S1, ESI†). Such a large deviation from coplanarity would be destructive for a long range delocalization of π -electrons along the polymer main chain, deteriorating the charge transport performance of the polymer. Therefore, it would be desirable if the side chains on the indigo units could be removed after the polymer film is solution processed to retrieve the highly coplanar geometry of the unsubstituted indigo units.

t-Boc is a well-known thermally removable functional group, which was recently used as a thermocleavable functionality for small molecule and polymer semiconductors.^{28,32} We designed and synthesized a D-A polymer, **PIDBDT**, whose repeat unit is comprised of a *t*-Boc-substituted indigo (ID) unit and a benzo[1,2-*b*:4,5-*b'*]dithiophene (BDT) unit (Scheme 1). The long branched 2-decyltetradecyloxy group on the BDT unit was used to provide additional solubilizing ability to render **PIDBDT** soluble. After thermal removal of *t*-Boc groups, the high coplanarity of the indigo units would be recovered. The starting material, compound **1** (Tyrian purple), was synthesized in one step in 73% yield,³³ which was substituted with the *t*-Boc groups using di-*tert*-butyl 3,3'-dioxo-[2,2'-biindolylidene]-1,1'-dicarboxylate in 82.7% yield following the literature method.³⁴ With *t*-Boc substitution, compound **2** could be easily dissolved and purified by recrystallization. The Stille coupling polymerization between **2** and (4,8-bis((2-decyltetradecyloxy)benzo[1,2-*b*:4,5-*b'*]dithiophene-2,6-diyl)bis(trimethylstannane) (**4**) in the presence of tris(dibenzylideneacetone)-dipalladium (Pd_2dba_3)/tri(*o*-tolyl)phosphine ($\text{P}(\text{o-tolyl})_3$) as a catalyst was carried out in chlorobenzene at 110 °C for 60 h. The obtained crude polymer product was subjected to consecutive Soxhlet extraction with acetone, hexane, and chloroform. The yield of the polymer extracted with chloroform is 62.8% after removing the oligomers by acetone and hexane.



Scheme 1 The synthetic route to **PIDBDT**. Reagents and conditions: (i) NaOH/acetone/r.t.; (ii) 4-dimethylaminopyridine/di-*tert*-butyldicarbonate/DMF/0 °C to r.t.; (iii) NaOH/Zn/H₂O/11-(bromomethyl)tricosane/tetrabutylammonium bromide/reflux; (iv) *n*-butyllithium/trimethyltin chloride/THF/−78 °C to r.t.; (v) $\text{Pd}_2\text{dba}_3/\text{P}(\text{o-tolyl})_3/110$ °C; (vi) heating at ≥ 170 °C.

Gel-permeation chromatography (GPC) with chlorobenzene as the eluent and polystyrene as the standard at 40 °C was used to determine the molecular weight of **PIDBDT**. The number average molecular weight (M_n) of the polymer fraction extracted with chloroform is 42.1 kDa with a polydispersity index (PDI) of 2.74.

The thermocleavable behaviour of the *t*-Boc groups in **PIDBDT** was examined by using thermogravimetric analysis (TGA) at 10 °C min^{−1} under nitrogen. As shown in Fig. 2, the polymer started to lose weight at ~ 170 °C and reached a flat region with a weight loss of $\sim 15\%$ at ~ 240 °C. This weight loss coincided with the calculated mass of the *t*-Boc groups ($\sim 15\%$) in

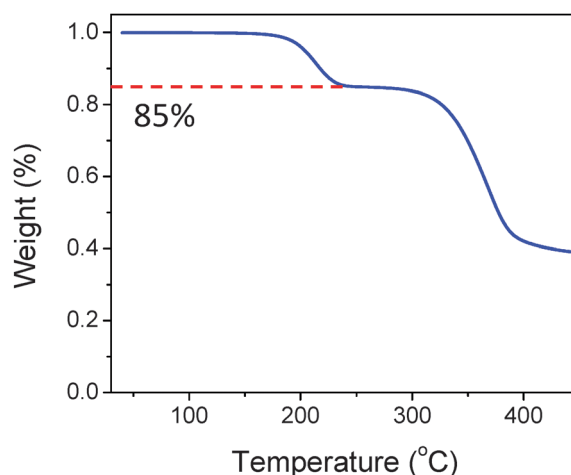


Fig. 2 TGA curves of **PIDBDT** at a heating rate of 10 °C min^{−1} under nitrogen.

PIDBDT, indicating that almost all the *t*-Boc groups were removed. At a higher temperature above $\sim 290^\circ\text{C}$, the polymer began to undergo a second abrupt weight loss. Since the indigo moiety is quite thermally stable (the melting point of indigo is $390\text{--}392^\circ\text{C}$),³⁵ the second decomposition step was probably due to the decomposition of the alkoxy-substituted BDT units.^{36–38}

Fig. 3 shows the X-ray diffractometry (XRD) measurements of the **PIDBDT** films annealed at 100, 150, 200 and 250°C for 1 h, respectively. No obvious diffraction peak was observed for the film annealed at 100°C . As the annealing temperature was increased to 150°C , a strong primary diffraction peak was observed at $2\theta = 3.95^\circ$ (corresponding to a *d*-spacing distance of 2.24 nm), indicating the significantly improved crystallinity of the polymer film. When the annealing temperature was further increased to 200°C , the primary peak intensified significantly. The *d*-spacing increased to 2.37 nm ($2\theta = 3.73^\circ$), which is likely a result of the backbone planarization. After being annealed at 250°C , the *d*-spacing increased further to 2.49 nm ($2\theta = 3.55^\circ$), but the intensity of the primary peak decreased probably due to partial decomposition of the alkoxy-substituted BDT units.^{36–38} It is reasonable to consider that the indigo units retrieved high coplanarity once the *t*-Boc groups were removed, which facilitated the formation of more ordered molecular packing. The observation of only the primary peaks in the XRD diagrams suggests that upon removal of the *t*-Boc groups the polymer chains adopted a layer-by-layer lamellar packing motif in thin films as observed for many other π -conjugated polymers.^{1,39} The primary peak represents the inter-lamellar distance.

The atomic force microscopy (AFM) measurements of the **PIDBDT** films revealed the changes in the surface morphology with increasing annealing temperature (Fig. 4). A very smooth surface (with a root-mean square (RMS) roughness of ~ 0.5 nm) with fine grains was observed for the film annealed at 100°C . As the annealing temperature increased to 150°C , small grains appeared and the surface roughness increased slightly (RMS roughness: ~ 1.5 nm). When the film was annealed at 200°C , the grains grew further and aggregated, forming fibre-like patterns.

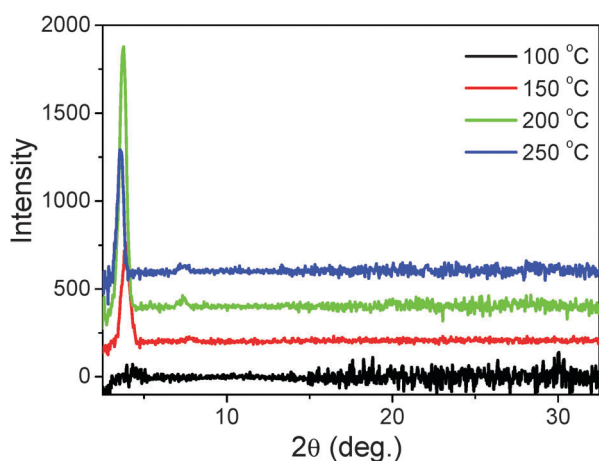


Fig. 3 XRD diagrams obtained from spin-coating polymer thin film on DDTS modified SiO_2 substrates annealed at 100, 150, 200 and 250°C .

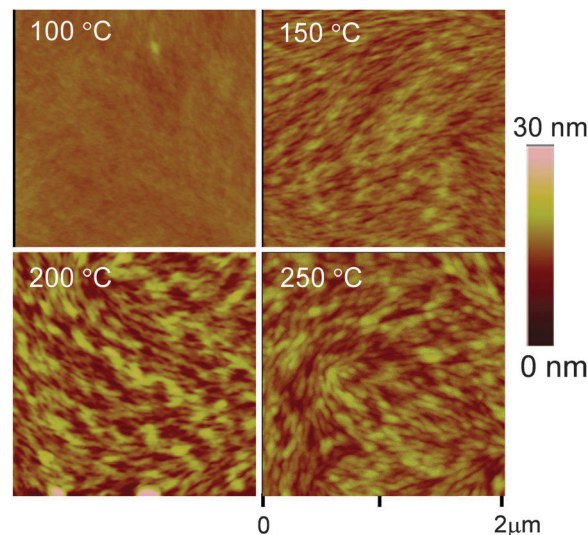


Fig. 4 AFM images ($2\ \mu\text{m} \times 2\ \mu\text{m}$) of polymer thin films (~ 70 nm) on dodecyltrichlorosilane (DDTS) modified SiO_2 substrates annealed at 100, 150, 200 and 250°C .

The RMS roughness increased to 3.2 nm. At a higher annealing temperature of 250°C , more distinct grains can be observed and the RMS roughness decreased to 2.2 nm.

The UV-vis absorption spectra of compounds **1** and **2** in dilute 1,1,2,2-tetrachloroethane (TCE) solutions are shown in Fig. 5a. The λ_{max} of compound **1** is 586 nm, which is in good agreement with the value of 585 nm reported in the literature.⁴⁰ The λ_{max} of **2** is at 545 nm, which blue-shifted for 40 nm. This is due to the twisting of this molecule caused by the *t*-Boc substitution as indicated by the simulation results discussed above. Fig. 5b shows the UV spectra of **PIDBDT** in dilute 1,2,4-trichlorobenzene before and after heating at 200°C for 1 h (and cooled to room temperature before the measurement). The large red shift (55 nm) in λ_{max} (from 585 nm to 641 nm) strongly indicated that the *t*-Boc groups were removed at 200°C , resulting in a more coplanar conformation of the polymer main chains in solution. Spectral changes of the polymer thin films on glass substrates annealed at different temperatures are shown in Fig. 5c. The spectrum of the 150°C -annealed film became obviously broader and red-shifted compared with the non-annealed ($\lambda_{\text{max}} = 587$ nm) and the 100°C -annealed films, indicating that the *t*-Boc groups are partially removed. For the 200°C -annealed film, a strong new peak at 658 nm appeared, suggesting the more extended π -conjugation realized by retrieving the high coplanarity of the unsubstituted indigo units upon removal of the *t*-Boc groups. The 200°C -annealed films could be dissolved in chloroform because the remaining large 2-decyltetradecyloxy groups on the BDT units could still solubilize the polymer to some extent. Further increasing the annealing temperature to 250°C resulted in a decrease in the intensity of the 658 nm peak, which might be caused by partial decomposition of the polymer main chains under such harsh conditions (250°C for 1 h). The colour changes of the polymer films can be clearly visualized as shown in Fig. 6. The optical band gap

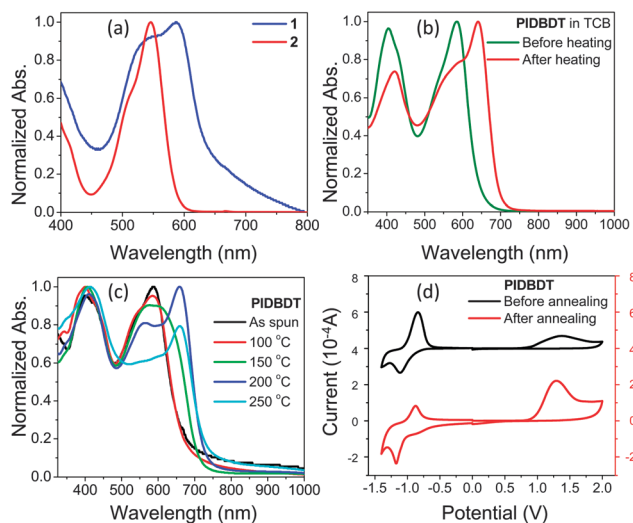


Fig. 5 UV-vis absorption spectra of (a) **1**, and **2** in TCE solutions, (b) a solution of **PIDBDT** in 1,2,4-trichlorobenzene (TCB) before and after heating at 200 °C for 1 h, and (c) **PIDBDT** films on glass substrates annealed at different temperatures for 1 h. (d) Shows the cyclic voltammograms of as-spun and annealed (200 °C/1 h) **PIDBDT** thin films measured in anhydrous CH_3CN solution using Bu_4NPF_6 as the electrolyte at a scan rate of 50 mV s^{-1} .

calculated from the onset absorption wavelength decreased from 1.85 eV for the non-annealed film to 1.68 eV for the 200 °C-annealed film, manifesting planarization of the polymer backbone due to the thermal removal of the *t*-Boc groups. The energy levels of **PIDBDT** were determined by cyclic voltammetry (CV) on polymer films spin coated on conductive indium tin oxide (ITO) substrates. The non-annealed **PIDBDT** film exhibited HOMO/LUMO levels of $-5.6 \text{ eV}/-3.9 \text{ eV}$ (Fig. 5d), respectively, using ferrocene as the reference (-4.8 eV).⁴¹ The CV curves of the polymer film annealed at 200 °C for 1 h were lowered to -5.8 eV and -4.2 eV , respectively. This suggests that the retrieved non-substituted indigo unit is a very strong electron acceptor building block. The band gap of $\sim 1.7 \text{ eV}$ determined from the CV curve of the 200 °C-annealed polymer film agrees with the value of 1.68 eV calculated from the onset absorption wavelength of the annealed film in the UV spectrum.

Bottom gate, bottom contact transistors with **PIDBDT** as a channel semiconductor were fabricated by spin-coating a **PIDBDT** solution in chloroform (5 mg mL^{-1}) onto a heavily n-doped Si/SiO₂ wafer patterned with gold source/drain electrodes (having a channel length of 30 μm and a channel width of 1 mm). Devices were annealed at 100, 150, 200 and 250 °C for 1 h, respectively, on a hot plate in a glove box filled with nitrogen.

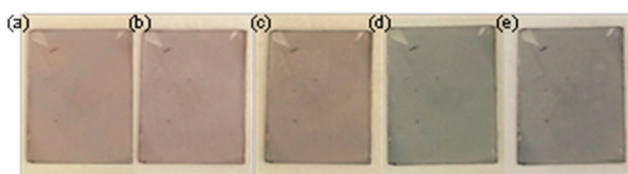


Fig. 6 **PIDBDT** films coated glass substrates before (a) and after annealing at (b) 100, (c) 150, (d) 200 and (e) 250 °C.

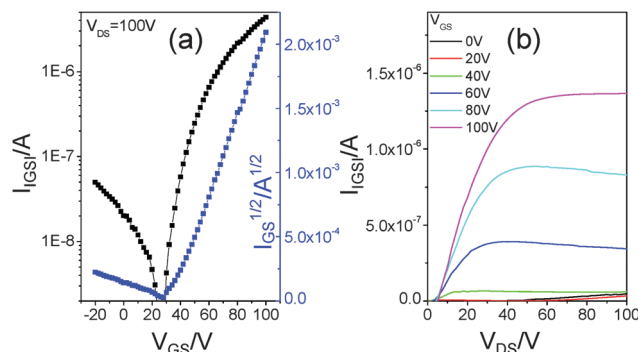


Fig. 7 Transfer and output curves of OTFT devices with **PIDBDT** thin films annealed at 200 °C for 1 h. Device dimensions: channel width (W) = 1 mm; channel length (L) = 30 μm .

No field effect transistor performance was observed for the polymer films annealed at 100 and 150 °C, mostly due to the highly twisted polymer backbone (with poor π -conjugation) and the disordered molecular packing of the polymer films. Devices with polymer films annealed at 200 °C for 1 h exhibited distinct n-channel electron transport behaviour, reaching the highest electron mobility of $5.7 \times 10^{-3} \text{ cm}^2 \text{ V}^{-1} \text{ s}^{-1}$ with current on-to-off ratios of $\sim 10^3$ (Fig. 7 and Table S2, ESI†). Apparently the charge transport of the 200 °C-annealed films was enabled by thermal removal of the *t*-Boc groups. The retrieved high coplanarity of polymer backbone and improved crystallinity of the films facilitated charge transport. Extremely weak hole transport characteristics (with the negligible on-current of $\sim 10^{-9} \text{ A}$) were observed in the hole accumulation mode. The exhibition of electron transport performance is due to the low-lying LUMO level (-4.2 eV) of the 200 °C-annealed polymer films. We found that the UV-vis spectra of the polymer films annealed at 200 °C for longer than 30 min remained very similar, suggesting the complete removal of the *t*-Boc groups (Fig. S8, ESI†). The film annealed for 30 min showed slightly lower mobility ($3.1 \times 10^{-3} \text{ cm}^2 \text{ V}^{-1} \text{ s}^{-1}$ in average), while a longer annealing time (3 h) did not further improve the mobility (Table S2, ESI†). The average electron mobility of the device annealed at 250 °C for 1 h dropped to $2.5 \times 10^{-3} \text{ cm}^2 \text{ V}^{-1} \text{ s}^{-1}$ probably due to partial decomposition of the polymer at such a high temperature as observed in its XRD and UV-vis spectra.

Experiment

Materials and instrumentation

4-Bromo-2-nitrobenzaldehyde was purchased from Oakwood Products. Other chemical reagents were purchased from Sigma Aldrich and used without further purification. 6,6'-Dibromo[2,2'-biindolylidene]-3,3'-dione (**1**),³³ benzo[1,2-*b*:4,5-*b'*]dithiophene-4,8-dione,⁴² 4,8-bis((2-decyltetradecyl)oxy)benzo[1,2-*b*:4,5-*b'*]dithiophene (**3**) and (4,8-bis((2-decyltetradecyl)oxy)benzo[1,2-*b*:4,5-*b'*]dithiophene-2,6-diyl)bis(trimethylstannane) (**4**)³⁷ were synthesized following the reported methods. NMR spectra were collected on a Bruker DPX 300 MHz spectrometer using tetramethylsilane (TMS, 0 ppm) as a reference. UV-vis spectra were obtained on a

Thermo Scientific GENESYS20 spectrophotometer. Cyclic voltammetry experiments were carried out on an electrochemical analyser CHI600E using an Ag/AgCl reference electrode, a Pt wire counter electrode, and a Pt foil working electrode in 0.1 M tetrabutylammonium hexafluorophosphate in dry acetonitrile under nitrogen at a scan rate of 50 mV s⁻¹. Ferrocene, which has a HOMO energy level of -4.8 eV,⁴¹ was used as the reference. Gel-permeation chromatography (GPC) measurements were performed on a Waters SEC with chlorobenzene as the eluent at 40 °C. A TGA Q500 (TA Instruments) system was used to conduct the thermogravimetric analysis (TGA) at a heating rate of 10 °C min⁻¹. A Bruker D8 Advance powder diffractometer with the standard Bragg-Brentano geometry using Cu K α radiation (λ = 1.5406 Å) was used to record the XRD diagrams of polymer thin films (~70 nm). The atomic force microscopy (AFM) morphological images of polymer thin films were obtained using a Dimension 3100 scanning probe microscope. The polymer film samples for the XRD and AFM measurements were prepared by spin-coating a polymer solution (10 mg mL⁻¹ in chloroform) on dodecyltrichlorosilane (DDTS) modified SiO₂/Si substrates, followed by annealing at selected temperatures.

Synthesis of 6,6'-dibromo-[2,2'-biindolinylidene]-3,3'-dione (1)³³

4-Bromo-2-nitrobenzaldehyde (2 g, 8.7 mmol) was dissolved in acetone (90 mL), followed by slow addition of water (100 mL). Then a 2 N aqueous NaOH solution was added drop-wise at room temperature to adjust the pH to 10. The mixture was stirred overnight at room temperature and filtered. The solid was washed with excess acetone and de-ionized (DI) water, and dried *in vacuo* to give a purple powder (1.32 g, 72.1%).

Synthesis of di-*tert*-butyl 6,6'-dibromo-3,3'-dioxo-[2,2'-biindolinylidene]-1,1'-dicarboxylate (2)³⁴

To a suspension of compound 1 (0.842 g, 2.0 mmol) and 4-dimethylaminopyridine (0.147 g, 1.2 mmol) in *N,N*-dimethylformamide (DMF) (5 mL) was added di-*tert*-butyldicarbonate (2.31 g, 10.6 mmol) in two portions at 0 °C. Then the mixture was stirred for 20 h at room temperature, during which time the color of the suspension changed from dark red to bright red. The product was isolated by filtration and the residue was washed with DMF and DI water and dried. Recrystallization of the solid from a mixture of chloroform/isopropanol gave a bright red powder (1.03 g, 82.7%). ¹H NMR (300 MHz, CDCl₃) δ 8.26 (s, 2H), 7.61 (d, J = 8.1 Hz, 2H), 7.37 (dd, J = 8.1, 1.5 Hz, 2H), 1.61 (s, 18H).

Synthesis of 4,8-bis((2-decyltetradecyl)oxy)benzo[1,2-*b*:4,5-*b'*]-dithiophene (3)³⁷

NaOH (0.6 g, 15.0 mmol) was added into a mixture of 4,8-dihydrobenzo[1,2-*b*:4,5-*b'*]dithiophene-4,8-dione (0.22 g, 1.0 mmol), zinc powder (0.143 g, 2.2 mmol), and water (5 mL) at room temperature. The mixture was refluxed for 1 h and then 11-(bromomethyl)-tricosane (1.3 g, 3.0 mmol) and tetrabutylammonium bromide (49 mg, 0.15 mmol) were added. After refluxing for an additional

8 h, the reaction mixture was cooled to room temperature and quenched with cold water. The mixture was extracted with diethyl ether (100 mL \times 2) and the ether layer was separated and dried over anhydrous sodium sulphate. After the solvent was removed, the residue was purified by column chromatography on silica gel with hexane to afford a yellow oil (0.627 g, 70.0%). ¹H NMR (300 MHz, CDCl₃) δ 7.47 (d, J = 5.6 Hz, 2H), 7.35 (d, J = 5.5 Hz, 2H), 4.16 (d, J = 5.3 Hz, 4H), 0.88 (t, J = 6.6 Hz, 12H).

Synthesis of 4,8-bis((2-decyltetradecyl)oxy)benzo[1,2-*b*:4,5-*b'*]-dithiophene-2,6-diyl)bis(trimethylstannane) (4)³⁷

Compound 3 (0.448 g, 0.5 mmol) was dissolved in dry tetrahydrofuran (THF) (7 mL) under argon. The solution was cooled to -78 °C and *n*-butyllithium (0.7 mL, 1.8 mmol, 2.5 M in hexane) was added drop-wise. After the mixture was stirred at room temperature for 1 h, trimethyltin chloride (0.239 g, 1.2 mmol) was added in one portion. The mixture was stirred at room temperature for 2 h and poured into water (200 mL). The mixture was extracted with diethyl ether and the organic layer was separated and dried over anhydrous sodium sulphate. After the solvent was removed, the residue was recrystallized from acetone twice to give a white solid (0.434 g, 71.0%). ¹H NMR (300 MHz, DMSO-*d*₆) δ 7.50 (s, 2H), 4.17 (d, J = 5.3 Hz, 4H), 0.88 (t, J = 6.6 Hz, 12H).

Synthesis of PIDBDT

To a 25 mL dry Schlenk flask was added 2 (0.0941 g, 0.15 mmol), 4 (0.185 g, 0.15 mmol) and tri(*o*-tolyl)phosphine (P(*o*-tolyl)₃) (3 mg, 0.012 mmol). After degassing and refilling argon 3 times, anhydrous chlorobenzene (5 mL) and tris(dibenzylideneacetone)-dipalladium (Pd₂dba₃) (2.8 mg, 0.003 mmol) were added under an argon atmosphere. The mixture was stirred for 60 h at 110 °C under argon before cooling to room temperature. After bromobenzene (0.5 mL) was added, the mixture was heated to 110 °C again and stirred for an additional 2 h. The cooled mixture was poured into methanol, and the precipitate was collected by filtration and subjected to Soxhlet extraction sequentially with acetone, hexane and chloroform. Yield: 63 mg (30%) from the hexane extract and 129 mg (63%) from the chloroform extract.

Fabrication and characterization of organic thin film transistors (OTFTs)

PIDBDT was characterized in a bottom-gate, bottom-contact OTFT structure (W = 1 mm; L = 30 μ m). A heavily n-doped Si wafer with a 300 nm thick SiO₂ layer was used as the substrate, where the conductive Si layer and the SiO₂ layer worked as the gate and the dielectric, respectively. The source/drain electrode pairs on the SiO₂/Si substrate were prepared *via* thermal evaporation of gold through a shadow mask. The substrate was cleaned using an ultrasonic bath with DI water, rinsed with acetone and isopropanol. After drying under a nitrogen flow, the substrate was merged in a DDTS solution (3% in toluene) for 15 min, followed by rinsing with toluene and drying under a nitrogen flow. A PIDBDT film with a thickness of ~30 to 50 nm was deposited on the substrate by spin coating a polymer solution in chloroform (5 mg mL⁻¹) at 3000 rpm for 60 s and

subsequently annealing at 100, 150, 200 and 250 °C for 1 h at each temperature in a glove box filled with nitrogen. The devices were measured after annealing at each temperature in the glove box in the absence of light using an Agilent B2912A Semiconductor Analyser. Carrier mobility in the saturation regime was calculated by using a slope obtained from linear fitting of the $(I_D)^{1/2}$ versus V_G according to the equation given below:

$$I_D = \left(\frac{WC_i}{2L} \right) \mu (V_G - V_T)^2$$

where I_D is the drain current, μ is the charge carrier mobility, C_i is the capacitance per unit area of the insulator (SiO_2 , 300 nm, $C_i = 11.6 \text{ nF cm}^{-2}$), and V_G is the gate voltage, respectively.

Conclusion

A novel indigo based polymer **PIDBDT** bearing thermocleavable *t*-Boc groups has been demonstrated to be a promising n-type semiconductor for organic thin film transistors. TGA confirmed the cleavage and removal of the *t*-Boc groups at > 170 °C. The resulting side chain-free indigo units could retrieve a highly coplanar geometry, which was substantiated by the UV-vis and XRD results. After thermal removal of the *t*-Boc groups, the resulting polymer showed a deep-lying LUMO level of -4.2 eV, indicating the very strong electron accepting ability of the unsubstituted indigo building block. As a result, stable electron transport with electron mobility as high as $5.7 \times 10^{-3} \text{ cm}^2 \text{ V}^{-1} \text{ s}^{-1}$ was achieved. Work on exploring other types of appropriate donors to improve the charge transport performance of this novel class of indigo-based polymers is in progress.

Acknowledgements

The authors thank the Natural Sciences and Engineering Research Council (NSERC) of Canada for the financial support (Discovery Grants No. 402566-2011) of this research.

Notes and references

- 1 B. S. Ong, Y. Wu, Y. Li, P. Liu and H. Pan, *Chem. – Eur. J.*, 2008, **14**, 4766–4778.
- 2 A. C. Arias, J. D. MacKenzie, I. McCulloch, J. Rivnay and A. Salleo, *Chem. Rev.*, 2010, **110**, 3–24.
- 3 H. Klauk, *Chem. Soc. Rev.*, 2010, **39**, 2643–2666.
- 4 A. Facchetti, *Chem. Mater.*, 2011, **23**, 733–758.
- 5 C. Guo, W. Hong, H. Aziz and Y. Li, *Rev. Adv. Sci. Eng.*, 2012, **1**, 200–224.
- 6 C. B. Nielsen, M. Turbiez and I. McCulloch, *Adv. Mater.*, 2012, **25**, 1859–1880.
- 7 E. Bundgaard and F. C. Krebs, *Sol. Energy Mater. Sol. Cells*, 2007, **91**, 954–985.
- 8 R. Kroon, M. Lenes, J. C. Hummelen, P. W. M. Blom and B. de Boer, *Polym. Rev.*, 2008, **48**, 531–582.
- 9 J. Chen and Y. Cao, *Acc. Chem. Res.*, 2009, **42**, 1709–1718.
- 10 Y. J. Cheng, S. H. Yang and C. S. Hsu, *Chem. Rev.*, 2009, **109**, 5868–5923.
- 11 P. L. T. Boudreault, A. Najari and M. Leclerc, *Chem. Mater.*, 2011, **23**, 456–469.
- 12 R. S. Kularatne, H. D. Magurudeniya, P. Sista, M. C. Biewer and M. C. Stefan, *J. Polym. Sci., Part A: Polym. Chem.*, 2013, **51**, 743–768.
- 13 I. Osaka, G. Sauve, R. Zhang, T. Kowalewski and R. D. McCullough, *Adv. Mater.*, 2007, **19**, 4160–4165.
- 14 Y. Li, S. P. Singh and P. Sonar, *Adv. Mater.*, 2010, **22**, 4862–4866.
- 15 Y. Li, P. Sonar, L. Murphy and W. Hong, *Energy Environ. Sci.*, 2013, **6**, 1684–1710.
- 16 W. Hong, B. Sun, C. Guo, J. Yuen, Y. Li, S. Lu, C. Huang and A. Facchetti, *Chem. Commun.*, 2013, **49**, 484–486.
- 17 M. S. Chen, J. R. Niskala, D. A. Unruh, C. K. Chu, O. P. Lee and J. M. J. Fréchet, *Chem. Mater.*, 2013, **25**, 4088–4096.
- 18 Z. Yan, B. Sun and Y. Li, *Chem. Commun.*, 2013, **49**, 3790–3792.
- 19 Y. He, W. Hong and Y. Li, *J. Mater. Chem. C*, 2014, **2**, 8651–8661.
- 20 Z. Cai, H. Luo, P. Qi, J. Wang, G. Zhang, Z. Liu and D. Zhang, *Macromolecules*, 2014, **47**, 2899–2906.
- 21 G. Sandberg, *Indigo Textiles: Technique and History*, A & C Black, Lark Books, London, Asheville, 1989.
- 22 P. E. McGovern and R. H. Michel, *Acc. Chem. Res.*, 1990, **23**, 152–158.
- 23 E. D. Glowacki, L. Leonat, G. Voss, M.-A. Bodea, Z. Bozkurt, A. M. Ramil, M. Irimia-Vladu, S. Bauer and N. S. Sariciftci, *AIP Adv.*, 2011, **1**, 42132–42136.
- 24 E. D. Glowacki, G. Voss, L. Leonat, M. Irimia-Vladu, S. Bauer and N. S. Sariciftci, *Isr. J. Chem.*, 2012, **52**, 540–551.
- 25 M. Irimia-Vladu, E. D. Glowacki, P. A. Troshin, G. Schwabegger, L. Leonat, D. K. Susarova, O. Krystal, M. Ullah, Y. Kanbur, M. A. Bodea, V. F. Razumov, H. Sitter, S. Bauer and N. S. Sariciftci, *Adv. Mater.*, 2012, **24**, 375–380.
- 26 Y. Kanbur, M. Irimia-Vladu, E. D. Glowacki, G. Voss, M. Baumgartner, G. Schwabegger, L. Leonat, M. Ullah, H. Sarica, S. Erten-Ela, R. Schwödiauer, H. Sitter, Z. Küçükyavuz, S. Bauer and N. S. Sariciftci, *Org. Electron.*, 2012, **13**, 919–924.
- 27 C. Guo, B. Sun, J. Quinn, Z. Yan and Y. Li, *J. Mater. Chem. C*, 2014, **2**, 4289–4296.
- 28 E. D. Glowacki, D. H. Apaydin, Z. Bozkurt, U. Monkowius, K. Demirak, E. Tordin, M. Himmelsbach, C. Schwarzwinger, M. Burian, R. T. Lechner, N. Demitri, G. Voss and N. S. Sariciftci, *J. Mater. Chem. C*, 2014, **2**, 8089–8097.
- 29 O. Pitayatanakul, T. Higashino, T. Kadoya, M. Tanaka, H. Kojima, M. Ashizawa, T. Kawamoto, H. Matsumoto, K. Ishikawa and T. Mori, *J. Mater. Chem. C*, 2014, **2**, 9311–9317.
- 30 M. J. Frisch, *Gaussian 09 Programmer's Reference*, Gaussian, 2009.
- 31 M. J. Frisch, *et al.*, *Gaussian 09*, 2009, see ESI† for the full citation.
- 32 J. Lee, A. R. Han, J. Hong, J. H. Seo, J. H. Oh and C. Yang, *Adv. Funct. Mater.*, 2012, **22**, 4128–4138.
- 33 P. Imming, I. Imhof and M. Zentgraf, *Synth. Commun.*, 2001, **31**, 3721–3727.

- 34 K. Ichimura, K. Arimitsu and M. Tahara, *J. Mater. Chem.*, 2004, **14**, 1164–1172.
- 35 K. Hunger, R. Hamprecht, P. Miederer, C. Heid, A. Engel, K. Kunde, W. Mennicke and J. Griffiths, *Industrial Dyes*, Wiley-VCH Verlag GmbH & Co. KGaA, 2004, p. 205.
- 36 Y. Zou, A. Najari, P. Berrouard, S. Beaupré, B. Réda Aïch, Y. Tao and M. Leclerc, *J. Am. Chem. Soc.*, 2010, **132**, 5330–5331.
- 37 Q. Shi, H. Fan, Y. Liu, J. Chen, L. Ma, W. Hu, Z. Shuai, Y. Li and X. Zhan, *Macromolecules*, 2011, **44**, 4230–4240.
- 38 J. Yuan, X. Huang, F. Zhang, J. Lu, Z. Zhai, C. Di, Z. Jiang and W. Ma, *J. Mater. Chem.*, 2012, **22**, 22734.
- 39 H. Sirringhaus, P. J. Brown, R. H. Friend, M. M. Nielsen, K. Bechgaard, B. M. W. Langeveld-Voss, A. J. H. Spiering, R. A. J. Janssen, E. W. Meijer, P. Herwig and D. M. de Leeuw, *Nature*, 1999, **401**, 685–688.
- 40 P. Friedländer, S. Bruckner and G. Deutsch, *Justus Liebigs Ann. Chem.*, 1912, **388**, 23–49.
- 41 B. W. D'Andrade, S. Datta, S. R. Forrest, P. Djurovich, E. Polikarpov and M. E. Thompson, *Org. Electron.*, 2005, **6**, 11–20.
- 42 H. Pan, Y. Li, Y. Wu, P. Liu, B. S. Ong, S. Zhu and G. Xu, *J. Am. Chem. Soc.*, 2007, **129**, 4112–4113.